# Evidence for Charge-Trapping Inducing Polymorphic Structural-Phase Transition in Pentacene

**ARTICLE** *in* ADVANCED MATERIALS · JANUARY 2015

Impact Factor: 17.49 · DOI: 10.1002/adma.201403556



**9 AUTHORS**, INCLUDING:

Masahiko Ando
Hitachi, Ltd.
**36** PUBLICATIONS **446** CITATIONS
SEE PROFILE

Hiroyuki Ishii
University of Tsukuba
**40** PUBLICATIONS **187** CITATIONS
SEE PROFILE

Takashi Minakata
Asahi Kasei
**12** PUBLICATIONS **84** CITATIONS
SEE PROFILE

Henning Sirringhaus
University of Cambridge
**278** PUBLICATIONS **24,945** CITATIONS
SEE PROFILE

# Evidence for Charge-Trapping Inducing Polymorphic Structural-Phase Transition in Pentacene

*Masahiko Ando,* Tom B. Kehoe, Makoto Yoneya, Hiroyuki Ishii, Masahiro Kawasaki, Claudia M. Duffy, Takashi Minakata, Richard T. Phillips, and Henning Sirringhaus*

The effects of interface intermolecular disorder in crystalline molecular semiconductors on the charge-carrier localization in crystalline pentacene transistors were investigated using in situ microRaman spectroscopy with theoretical simulations. Trapped charge-induced transformations of pentacene polymorphs were observed for the first time and the molecular dynamics (MD) simulations revealed that the charge should be localized in pentacene molecules with static intermolecular disorder along the long axis. Quantum chemical calculations of the intermolecular transfer integrals suggested the disorder was large enough to induce Anderson-type localization.

There has been tremendous progress made in producing highly crystalline films of molecular semiconductors from solution that provide high carrier mobility, above 1 $cm^2\ Vs^{-1}$, for a range of applications, and potentially low-cost and large-area processability.[1,2]

A theoretical understanding of the charge transport mechanism in molecular semiconductors has been also developed to shed light on the disorder, either dynamic or static, which plays decisive roles in determining the carrier localization/delocalization properties of the organic semiconductors.[3–7] It is theoretically predicted that dynamic and static disorder induce transient and continuous localization of charge carriers, respectively.[6,7] Notably, the transient localization theory successfully reconciled the contradictory experimental observations of band-like temperature dependence of the mobility and the very short charge-carrier localization length, recently observed by several techniques.[8]

Dr. M. Ando, Dr. M. Kawasaki
Central Research Laboratory, Hitachi, Ltd.
7-1-1 Omika, Ibaraki 319-1292, Japan
E-mail: masahiko.ando.ph@hitachi.com
Dr. T. B. Kehoe, Dr. C. M. Duffy,
Prof. R. T. Phillips, Prof. H. Sirringhaus
Cavendish Laboratory
JJ Thomson Avenue, Cambridge CB3 0HE, UK
Dr. M. Yoneya
Nanosystem Research Institute
National Institute of Advanced Industrial Science and Technology
1-1-1 Umezono, Tsukuba 305-8568, Japan
Prof. H. Ishii
Institute of Applied Physics and Tsukuba Research Center
for Interdisciplinary Materials Science
University of Tsukuba
1-1-1 Tennodai, Tsukuba, Ibaraki 305-8573, Japan
Dr. T. Minakata
Asahi-Kasei Corporation
R&D Centre, Samejima
Fuji, Shizuoka, Japan

**DOI: 10.1002/adma.201403556**

In contrast, continuous localization or charge-trapping induced by static disorder is not so much reported so far[9–12] despite that device performance is often discussed based on the existence of static disorder.[13] It is enormously difficult to identify which specific kinds of disorder should affect the charge-carrier localization because of the complex molecular microstructures encountered by charges moving through the bulk of a van der Waals bonded molecular system or along the interface with a gate dielectric. Therefore, a full microscopic understanding of the structure–property relationship for localization at a molecular scale remains elusive.

Here, we provide evidence for continuous localization (charge-carrier trapping) induced by a specific intermolecular disorder in molecular semiconductors detected by in situ microRaman spectroscopy under gate bias-stress, light-illumination, and thermal-annealing cycles. The microscopic origin of the charge-induced intermolecular disorder and the relationship to the charge localization have been investigated using MD simulation of multilayer molecular system,[14] combined with quantum chemical calculations.[7] The MD simulation revealed that the thermal molecular fluctuations were supprVessed at the interface and the charge-trapping molecular disorder was frozen at room temperature. Fluctuations of the transfer integrals of the MD-simulated molecular configuration are shown to be large enough to reach the condition for disorder-induced Anderson-type localization to occur.[6,7]

We utilized the benchmark molecular semiconductor pentacene ($C_{22}H_{14}$), one of the most thoroughly investigated materials. Zone-cast pentacene (ZCPEN) films[15] were used as a model system for the present study. The ZCPEN films were composed of two kinds of polymorphs with quite different degrees of intermolecular disorder along the long molecular axis[14] as shown in **Figure 1**c where the HT- and LT-polymorph structures of pentacene are shown. The herringbone arrangement of molecules in the layers are virtually identical in both polymorphs, whereas their interlayer stacking differs significantly.[14,22] The molecules are colinearly aligned between adjacent layers in the LT-phase (blue dotted line), whereas the molecules in adjacent layers are shifted in the HT-phase (red dotted line). Therefore, fluctuation of the pentacene molecule along the long molecular axis direction is allowed in the aligned LT-phase, whereas it is suppressed in the shifted HT-phase due to the steric hindrance between the adjacent molecules. Our previous MD simulation indicated that the fluctuation in the LT-phase is almost one order of magnitude larger than that in the HT-phase (see inset of Figure 4c).[14] Therefore, it is suitable to investigate the microstructural disorder versus charge localization relationship which has been theoretically investigated.[3–7] Zone-cast films form aligned elongated crystal grains

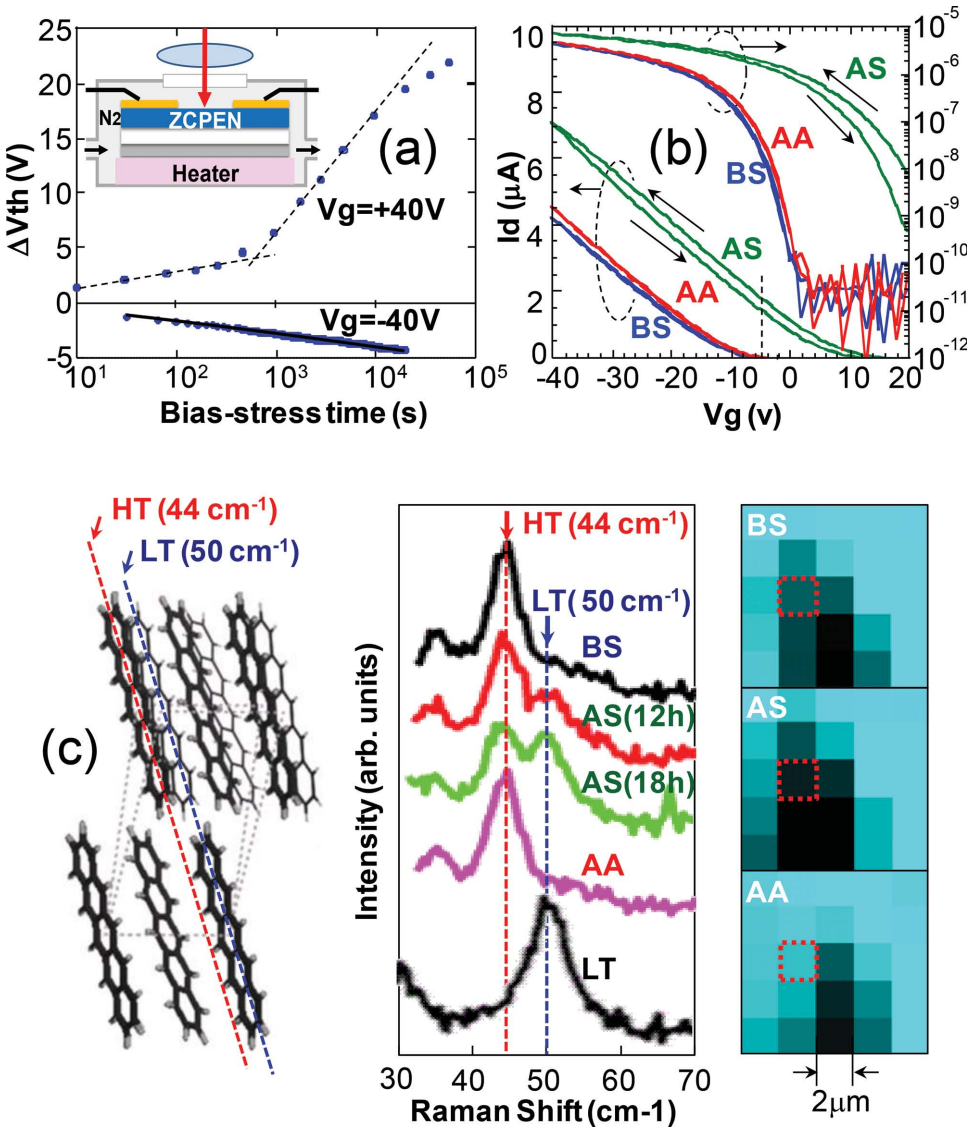


**Figure 1.** a) $V_{th}$ shift ($\Delta V_{th}$) during positive and negative gate bias stress, sectional device structure shown in the inset, b) Transfer *I–V* characteristics in linear and log plots for before and after gate bias stress (BS and AS, respectively) and after annealing at 130 °C (AA), c) From left to right: HT- and LT-polymorph structures of pentacene single crystal viewing along a-axis, the parallelograms correspond to the unit cells. Lower row bold: molecules of both structures, upper row bold: molecules of HT-phase; upper row regular: molecules of LT-phase. 44 $cm^{-1}$ is characteristic Raman peak for HT, 50 $cm^{-1}$ is that for LT; intermolecular vibration Raman peaks for BS, AS, and AA stages; corresponding Raman mappings (see text), dotted white square indicate measuring points of the Raman peaks shown in the middle.

many micrometers in size and therefore we can eliminate the effects of grain boundaries[10,12] which make characterization complicated and increases the sensitivity to impurities such as oxygen and water molecules. The effects of these impurities on charge trapping under prolonged gate bias stress can be reduced further by thermally annealing the ZCPEN in a nitrogen atmosphere.[16] The ZCPEN growth process was carried out with the substrate maintained at 180 °C in a dry nitrogen environment as described elsewhere.[15] Devices (inset of Figure 1a) were made with a 100 nm single layer of ZCPEN on a bilayer dielectric consisting of 70 nm of divinylsiloxane-bisbenzocyclobutene (BCB) on 300 nm of $SiO_2$ and with a highly-doped silicon substrate as the gate. 15 nm thick gold source and drain electrodes were evaporated on to the ZCPEN through a shadow mask to make top contact thin film transistors (TFTs) with a channel length of 20 μm, oriented so that the channel was parallel to the zone-casting direction. Prior to performing the bias stressing routine the devices were annealed at 130 °C in nitrogen for 1 h to stabilize the device performance. Field-effect mobilities upto 0.7 $cm^2$ $Vs^{-1}$ were achieved. After bias stressing the devices, which degrades the performance, the same annealing conditions were used to recover the device performance to the original level.

Raman spectroscopy permits identification of pentacene polymorphs with micrometer resolution.[17,18] ZCPEN films have medium- to long-range order of single crystals. To evaluate the degree of intermolecular disorder in ZCPEN films, we studied the low-energy intermolecular vibrational modes in

the Raman spectra between 10 and 200 $cm^{-1}$ which are sensitive to the intermolecular packing. In situ Raman and current–voltage (I–V) measurements were performed with the device in a nitrogen atmosphere (Linkam LTSE350: inset of Figure 1a). A HeNe laser (<500 μW, 632.8 nm) was focused to ≈1 μm on the pentacene surface, and Raman spectra from 10 to 1700 $cm^{-1}$ were obtained using a triple-grating spectrometer (Horiba Jobin Yvon T64000). An *X*–*Y* stage enabled Raman mapping with a 2 μm pitch. To investigate the correlation between the microstrucure and charges trapped in pentacene, the Raman spectrum of the pentacene film was measured before and after a prolonged application of bias stress. Such a bias stress resulted in charge trapping as indicated by a pronounced shift of the transistor turn-on threshold voltage. Charges were detrapped either by annealing or by photoexcitation of the pentacene[19] with light in the 1–3 eV spectral range (avoiding sample heating) from a xenon lamp filtered with indium tin oxide coated glass. For inducing gate bias-stress effects, a gate voltage ($V_g$) = ± 40 V was continuously applied for up to 18 h with the drain voltage ($V_d$) kept at –5 V.

Our ZCPEN transistors exhibit unsymmetrical threshold voltage shifts ($\Delta V_{th}$), dependent on the polarity of the gate bias stress as shown in Figure 1a. In the case of negative bias stress at $V_g$ = –40 V with hole accumulation at the interface, $\Delta V_{th}$ is relatively small at 5 V for 10 h stress. These data are well fitted by the expression (log *t*)$\lambda$ where *t* is the stress time and $\lambda$ = 1.2 (black solid line), indicating that the negative $V_{th}$ shift is due to the tunnelling injection of holes into the dielectric.[21] In the case of positive bias stress at $V_g$ = +40 V, the initial $\Delta V_{th}$ for a stress time up to about *t* = 1000 s has the same (log *t*)$\lambda$ tendency as for the negative bias stress, indicating the tunneling injection of electrons into the gate dielectric. However, the rate of $\Delta V_{th}$ remarkably begins to increase for stress times exceeding 1000 s. Our previous investigation revealed that a certain amount of time is necessary to accumulate electrons at the interface,[16] as electrons are injected from nonOhmic contacts. During the charge trapping time for relatively large $\Delta V_{th}$ electrons sufficiently accumulate at the interface and screen the electric field from the gate. As the absolute value of the electric field applied to the dielectric is the same for positive and negative gate bias voltages, it seems that electrons contributing to the large $\Delta V_{th}$ are not trapped in the dielectric but in the pentacene as we will discuss further below.

The positive $\Delta V_{th}$ due to trapped electrons is reversible as shown in Figure 1b, where $I_d$–$V_g$ curves are plotted linearly (left ordinate) and logarithmically (right ordinate). Data are shown for both upward sweeping of the gate bias, and for the subsequent downsweep. There is a clear threshold in the logarithmic plots, and this threshold shifts from initial state before stress (BS) to that after bias stress (AS). After thermal annealing at 130 °C in a nitrogen atmosphere (AA), the $I_d$–$V_g$ characteristic returns to very close to its original form.

Evidence for the transformation of the microstructure of pentacene under positive bias stress and annealing are shown in Figure 1c. Figure 1c (left frame) shows how the herringbone stacking of the pentacene molecules differs in the two structures. The first layer of the two structures (bottom of the figure) is the same, but the low-temperature (LT) form has the molecules aligned in the second layer (see blue dashed line) whereas the high-temperature form (HT) shows an offset in the second layer (see red dashed line). Furthermore, details are discussed by Siegrist et al.[22]. The HT-form has a vibrational mode at 44 $cm^{-1}$, whereas the corresponding mode in the LT-form is shifted to 50 $cm^{-1}$.[17] The transformation between the two structures under bias stress emerges from the Raman spectra clearly, as seen in the middle panel of Figure 1c, which shows the growth of the LT Raman signature after 12 and 18 h of bias stress, and its elimination by annealing. The two forms show differing steric hindrance of fluctuation of the molecular position along long molecular axis. Our previous MD simulation indicated that such fluctuation in the LT-phase is almost one order of magnitude larger than that in the HT-phase (see inset of Figure 4c).[14] A structural map generated by assigning a grayscale to the ratio of intensities of the Raman peaks at 44 and 50 $cm^{-1}$ for a 10 × 10 $\mu m^2$ area of the sample, as seen in the right panel of Figure 1c, indicates that the ZCPEN films are composed of majority regions of HT-phase (bright regions) with small amounts of LT-phase (dark regions) dispersed within the HT-matrix. The coexistence of the two polymorphs has already been reported in single crystal and powder forms[22]; the present results extend this to 100 nm thick thin films.

Remarkably, it was found that the area in the LT-phase tends to spread under gate bias stress and contract under thermal annealing. The Raman spectra measured in the transitional region (a red dotted square on the map) clearly show the reversible transformation between HT-, mixed-, and HT-phase-induced by gate bias stress and annealing. This is unlikely to be due directly to electric field, as the electric field applied to the gate is screened from the pentacene by electrons accumulated at the interface. A potential mechanism is electrostriction of the polymer dielectric BCB, which could initiate transformation of the pentacene through mechanical stress. This explanation can be eliminated, since it implies that similar transformations should occur with the bias reversed, and these are *not* observed as shown in Figure 1a. We propose, therefore, that the reversible transformation is due to electrons being trapped and detrapped in the pentacene at the interface.

A test of this model is provided by direct photoexcitation of the pentacene to release the trapped electrons. **Figure 2** shows the variation of the intensities of the LT and HT Raman peaks and the observed accumulated electron density, $\Delta Q$, following continuous gate bias stress at $V_g$ = +40 V and $V_d$ = –5 V. The gate bias stress is turned off at *t* = 0 s and $\Delta Q$ at the interface and the Raman peak intensities in the transitional region (1 μm spot in the red dotted square in Figure 1c) were monitored in situ as a function of time. The initial decrease of $\Delta Q$ in the dark until *t* = 4300 s is due to free electrons accumulated by gate bias being released from shallower states at the interface. It is surprising that in this period, after switching off the bias stress, the transformation from the HT- to the LT-phase clearly continues. Since the external field has been removed, this observation confirms that the transformation is not due to the external electric field but must be connected in some way to the presence of electrons accumulated at the interface. We speculate that some of the released electrons might diffuse into the bulk and enhance the transformation. The residual $\Delta Q$ at *t* = 4300 s should correspond to deeply-trapped electrons at the interface.

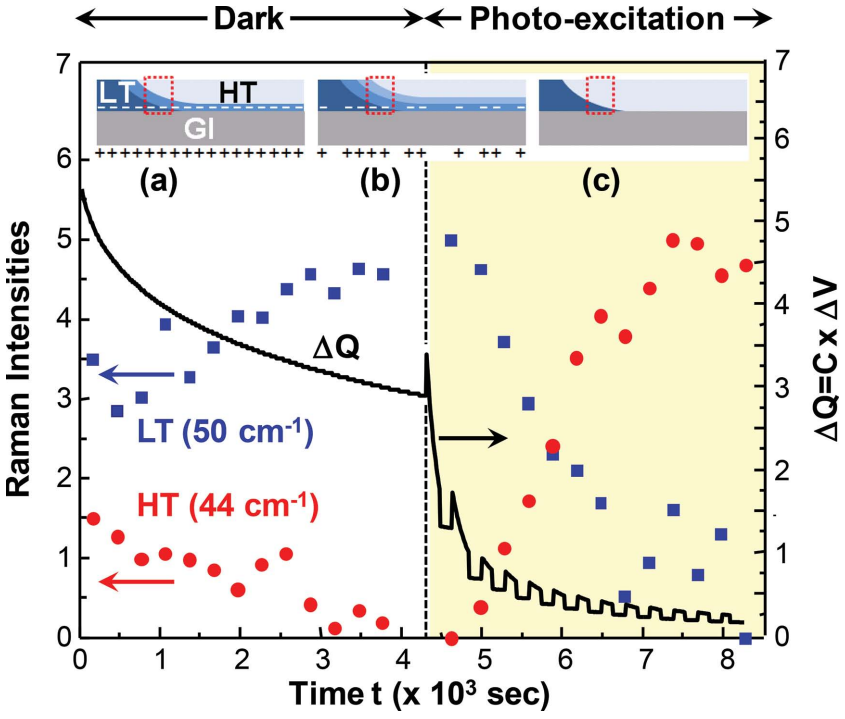


**Figure 2.** Trapped charge density $\Delta Q$ and Raman peaks intensities for HT- and LT-polymorphs (HT (44 $cm^{-1}$), LT (50 $cm^{-1}$)) as a function of time after 18 h continuous gate bias stress at $V_g = +40$ V, $V_d = -5$ V. Gate-bias stress is turned off at time $t = 0$ s, after which the current recovery is monitored periodically by pulsed current measurement at the same voltage conditions. Light illumination is started at $t = 4300$ s to release trapped electrons in pentacene. Sectional images of polymorph distribution in pentacene films are schematically shown as insets; a) during bias stress: left LT-phase penetrating into right HT-phase with accumulated electrons (–) at gate insulator interface, the extended LT-phase colored in lighter blue, b) after bias stress is turned off: trapped electrons (–) remaining at interface with LT-phase further extending into LT-phase as colored in more lighter blue, and c) after light illumination: extended LT-phase transforming to LT-phase again after all trapped electrons released by photoexcitation, red dotted square corresponds to the section of the area shown in red dotted square in the right panel of Figure 1c.

After $t$ = 4300 s the pentacene was repeatedly illuminated for periods of 150 s with light with photon energies between 1 and 3 eV. Raman spectra were recorded during the 150 s interval between illuminations (the discontinuous jumps just after illumination are due to photocurrent components, and the dips correspond to the dark intervals for Raman measurements). $\Delta Q$ reduces down to 30% of the initial value after a total of 300 s illumination. The intensities of the Raman peaks are clearly correlated with the $\Delta Q$ decrease. The intensity of the LT peak at 50 $cm^{-1}$ decreases while the intensity of the HT peak at 44 $cm^{-1}$ increases indicating a recovery to the initial HT-phase after about 4000 s illumination. Since the electron traps in pentacene are known to be distributed between the energy levels 1.8–2.5 eV in the gap states,[19] the illumination with photon energy of 1–3 eV should release the trapped electrons in pentacene at the interface and play a role in the transformation from the LT- to the HT-phase. These results clearly indicate that electrons are trapped in the pentacene under positive gate bias stress and stabilize the LT-phase usually unstable in ZCPEN films on a dielectric surface. Although the charge-induced transformation is observed only at transitional regions between the two polymorphs in the present microRaman spectroscopy, we expect it should happen uniformly at the pentacene/dielectric interface as shown schematically in insets of Figure 2, since the charges have been shown, by Kelvin probe measurements,[16] to be uniformly trapped.

We now turn to microscopic simulations which can inform our interpretation of the experimental results. We apply a flexible all-atom MD model to evaluate the effects of charge trapping on structural transformation. All simulations have been performed for a temperature of 293 K and pressure of 1 atmosphere as detailed elsewhere.[14] The stabilization of the LT-phase by electrons trapped in the pentacene at the interface, suggested by the experimental results, is also reproduced by our MD simulation as shown in **Figure 3**. The Figure shows the simulated time evolution of the nearest neighbor interlayer molecular distance, $d_1$ (as defined in the inset), for a pentacene multilayer system. Three cases are compared, (a) when the first pentacene layer in the structure is without charges (black), (b) when the first pentacene layer is charged up with electrons and then discharged at $t = 2$ ns (blue), and (c) when the dielectric surface is charged up with electrons (cyan). In case (b) a total of 25% of the pentacene molecules in the first layer are randomly selected and each of the selected molecules is charged up with an elementary charge. The charge distribution on the dielectric surface for case (c) is built up from the charged-up first layer of pentacene by burying the same charges into the dielectric surface. Snapshots of the structures with the charged-up first layer of pentacene at $t = 0$, just before discharge at $t = 2$ ns, and after discharge are shown from left to right in the upper panel. All structures are viewed along the a-axis and three and a half layers are shown, out of a total of 12 simulated layers. The value of $d_1$ is a good parameter for distinguishing between the LT-phase ($d_1$ = 1.45 nm) and the HT-phase ($d_1$ = 1.52 nm). In the case of pentacene without charges (black line), the LT-phase as the starting structure abruptly transformed to the HT-phase with a time constant of 56 ps as previously shown in our earlier MD simulation.[14] However, the blue line shows that the LT-phase is stabilized by electrons trapped in the pentacene, and the discharge applied at $t$ = 2 ns clearly removes the stabilizing effect—the structure again abruptly changes to the HT-phase. In the case of the charged-up dielectric surface (cyan line), the LT-phase is not stabilized and is transformed to the HT-phase as in the case without charges. These results indicate that it is necessary for the electrons to be trapped in the pentacene molecules at the interface and not in the dielectric surface in order to stabilize the LT-phase during the gate bias stress.

Our previous MD simulation revealed that large molecular fluctuations along the long molecular axis stabilize the LT-phase in the bulk. However, the longitudinal fluctuation is suppressed on the dielectric surface and the destabilized LT-phase transforms into the HT-phase.[14] Shown in the upper panel

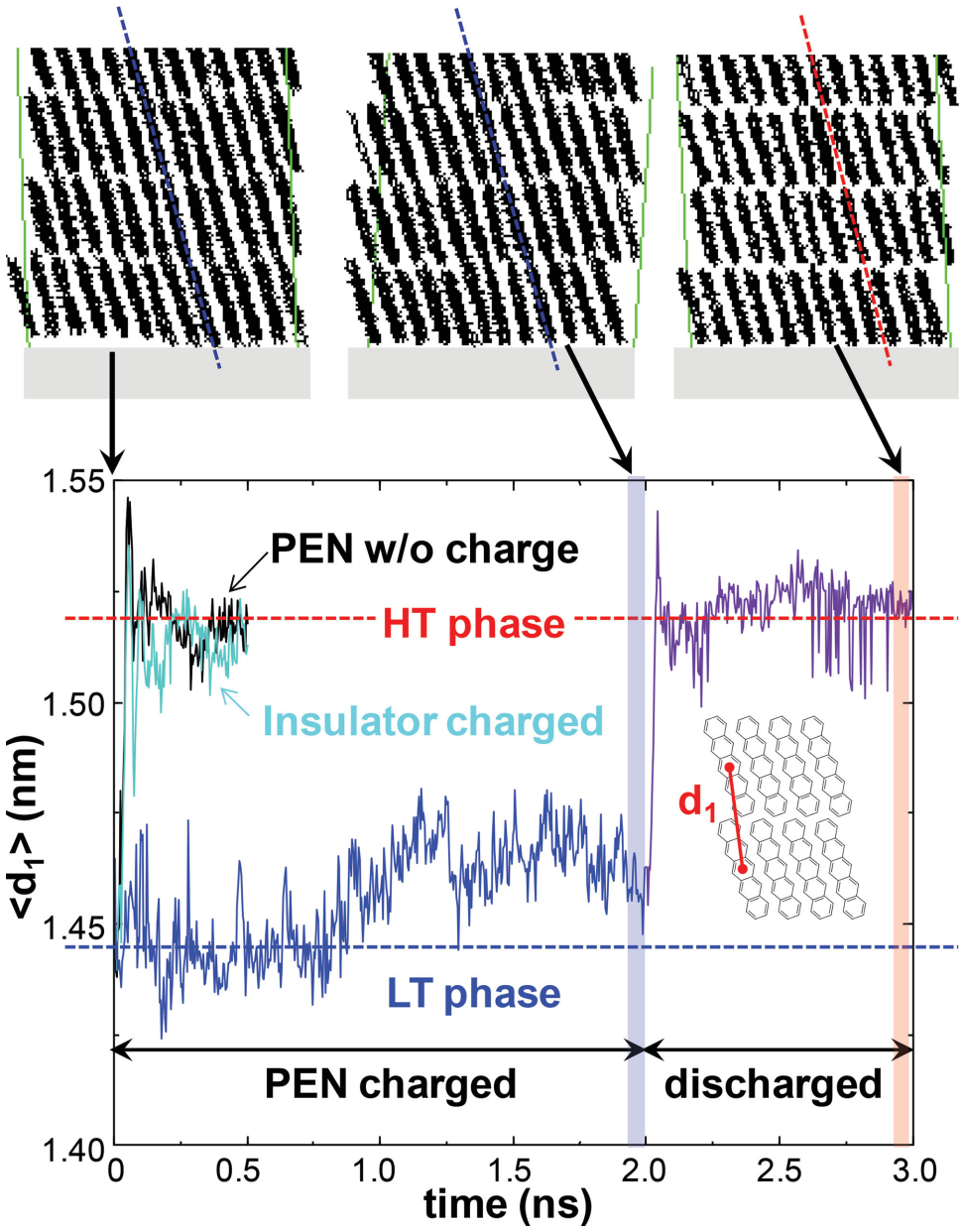


**Figure 3.** Simulated distance of nearest neighbor molecules in the adjacent layers, d1, as a function of time, representing time evolution of the LT-phase; charged pentacene first monolayer (blue), no charge (black), and charged dielectric surface (sky blue). LT-phase transformed into HT-phase when pentacene first layer is discharged at $t = 2$ ns. The structure at $t = 0$, just before discharge, and after discharge are shown from left to right. Three and a half layers from total 12-simulated layers are shown, all structures viewed from *a*-axis.

of Figure 3 are overlap images of many pentacene wire-frame models, which give a means of visualizing the amount of fluctuation of the pentacene molecules in each polymorph. In the charged-up LT-phase (left and middle), the pentacene images make interlayer connections and the layers are undulated. This means that the large longitudinal fluctuation is preserved and it stabilizes the charged-up LT-phase even on the dielectric surface. In contrast, clear interlayer spacing and substantially flat layers of the pentacene wire-frame model images in the HT-phase after discharge (right) indicates that the longitudinal fluctuation cannot be preserved without charge localization in the pentacene molecules.

By estimating the longitudinal fluctuation preserved in the charged-up LT-phase spatiotemporally, the fluctuation was found to be "static" disorder and large enough to induce Anderson-type charge localization. This is explained in the following with the aid of **Figure 4**, where intermolecular configurations of the first layer pentacene molecules before and after discharge were picked up from the middle and right in the upper panel of Figure 3 and investigated in more detail. A snapshot of the first layer pentacene molecules ($12 \times 7 = 84$ molecules) in the a–b plane and b–c plane for the charge stabilized LT-phase and for the HT-phase after discharge is shown in Figure 4a,b, respectively. The relative displacement along the long molecule

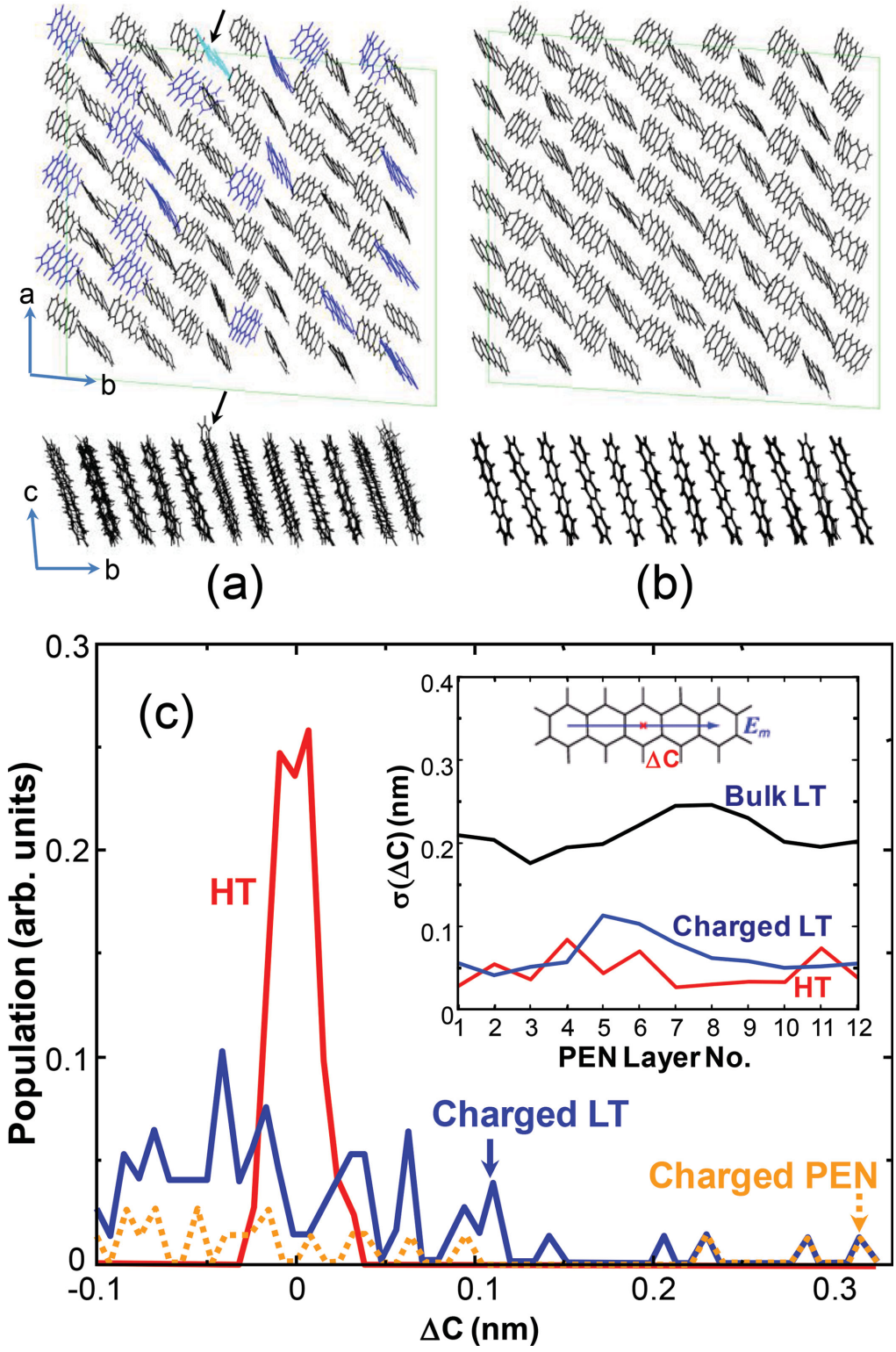


**Figure 4.** a) (from top to bottom) A Snapshot of charged pentacene first layer 12 × 7 molecules in the a–b plane (charged molecules colored in blue) and the a–c plane (LT-phase), b) those for discharged pentacene first layer (HT-phase), c) deviations of the pentacene center co-ordinates along the long molecular axis (ΔC) for charged LT-phase (blue) and those for HT-phase transformed after discharge (red). Inset shows the root-mean-squared fluctuations of the pentacene center coordinates (σ(ΔC)) along the long molecular axis direction averaged over each twelve layer of the film on the dielectric surface for charged LT-phase (blue), transformed HT-phase after discharge (red), and bulk LT-phase[14] for comparison. The Δ*C* for only the charged-up molecules is shown in orange dotted line.

axis, $\Delta C = C - \langle C \rangle$ is parallel to the c-axis, where $\langle C \rangle$ is the time average for the 40 ps period shown in the shaded area in Figure 3. There are negligible molecular displacements in the a–b plane preserving the herringbone configuration. However the $\Delta C$ for the charged-up LT-phase is remarkably high in contrast to that for the HT-phase, as quantitatively shown in Figure 4c. The $\Delta C$ for the HT-phase (red) is confined to values between –0.02 and +0.03 nm while the $\Delta C$ for the charged-up LT-phase (blue) is dispersed over the range –0.1 to over +0.3 nm almost one order of magnitude higher than that for the HT-phase (the unsymmetrical smaller dispersion in the negative direction is due to the existence of the hard dielectric surface). Furthermore, the $\Delta C$ dispersion in the charged-up LT-phase is found to be of a static rather than dynamic character, since the standard deviation of the $\Delta C$, $\sigma(\Delta C)$, is much smaller than the $\Delta C$ dispersion, as shown in the inset of Figure 4c where the $\sigma(\Delta C)$ for the 40 ps time period averaging over 84 molecules in each layer are shown from the 1st to the 12th layer. In both the HT- and the charged-up LT-phase, $\sigma(\Delta C)$ of the first monolayer (No.1) is equal to or less than 0.05 nm. In contrast, the $\Delta C$ in the bulk LT-phase without charges is almost six times larger than $\sigma(\Delta C)$, thus the larger $\Delta C$ is considered to be static. This is visually illustrated in the snapshot of the pentacene molecules shown in Figure 4a, where in the group of molecules in the sixth position from the left, the top benzene ring (indicated by the arrow) of the pentacene with the largest $\Delta C$ at 0.3 nm (Figure 4c) appears above the level of the surrounding molecules, as the amount of the displacement coincides with a benzene-ring diameter.

The large static displacement collectively occurs among the colinearly aligned pentacene molecules in the LT-phase, since a displaced molecule in the first monolayer pushes all the colinearly aligned adjacent molecules. This collective displacement should stabilize or pin the LT-phase even on a dielectric surface, as the displaced molecules are inserted in the adjacent layers and these "anchor" molecules prevent transformation into the HT-phase in which molecules in adjacent layers should be shifted as shown in the upper right panel of Figure 3. Based on this pinning mechanism of the charged-up LT-phase, the relatively high charge density (25%) is only necessary to be accumulated at locally disordered regions such as LT- and HT-phases boundaries as observed in grain boundaries in the vacuum sublimed pentacene thin films.[10]

It should be stressed that there is strong correlation between the occurrence of the large static displacement along the long axis and the charged molecules as shown in Figure 4a (charged molecules colored in blue) and Figure 4c. The $\Delta C$ for only the charged-up molecules is shown by the orange dotted line and all the three molecules with large positive $\Delta C$ exceeding 0.2 nm are charged-up ones. The large static and frozen disorder of the charged-up LT molecular configuration depends on a subtle balance between van der Waals force between molecules, their interaction with the substrate, and Coulomb forces between localized charges at the interface, affected by thermal molecular fluctuations. As the molecular fluctuation is leveled and suppressed by the interaction with the flat dielectric substrate as shown in our previous MD simulation without charges,[14] the origin of the static disorder is considered to be induced by the Coulomb repulsion between localized charges (electrons in the present case). Thus, our MD simulation revealed that (1) charges should be localized in the pentacene molecules in order to stabilize the LT-phase on a dielectric surface as experimentally observed (Figure 3), and (2) the localized charges induce the longitudinal intermolecular static disorder (Figure 4). Since, in the Anderson model the introduction of random and uncorrelated static disorder inevitably results in charge localization in 1D and 2D systems,[23] the static disorder in the charge-trapping LT-phase as revealed by the MD simulation also should have the potential to continuously localize the trapped charges. For sufficiently small polaron binding energy $E_b$ (≈45 me V for pentacene) the main origin of carrier localization is not small polaron formation, but disorder or fluctuations in the transfer integrals.[24,25]

The transfer integrals were calculated for the two MD-simulated molecular configurations of the first monolayer.[20] Two face-to-edge pentacene molecular pairs B and C in Figure 1 of ref. [24] were selected for calculating the transfer integrals for the monolayer since it has been shown that this pair, having higher values for the transfer integrals compared with other unequivalent pairs, contributes more to the charge transport.[24] The transfer integral values were averaged over 71 or 72 pairs in our 84 molecules. For the charged-up LT-phase the average transfer integral $V$ and standard deviation $\sigma$ due to static disorder for pairs of molecules were $V_B(\mathrm{LT}) = 258\ \mathrm{cm}^{-1}$, $\sigma_B(\mathrm{LT}) = 460\ \mathrm{cm}^{-1}$, $V_C(\mathrm{LT}) = 210\ \mathrm{cm}^{-1}$, $\sigma_C(\mathrm{LT}) = 500\ \mathrm{cm}^{-1}$. For the HT-phase after discharge, $V_B(\mathrm{HT}) = 419\ \mathrm{cm}^{-1}$, $\sigma_B(\mathrm{HT}) = 411\ \mathrm{cm}^{-1}$, $V_C(\mathrm{HT}) = 411\ \mathrm{cm}^{-1}$, $\sigma_C(\mathrm{HT}) = 347\ \mathrm{cm}^{-1}$. Comparing sum values of B and C, the larger $\sigma(\mathrm{LT}) = \sigma_B(\mathrm{LT}) + \sigma_C(\mathrm{LT})$ and the smaller $V(\mathrm{LT}) = V_B(\mathrm{LT}) + V_C(\mathrm{LT})$ make $\sigma(\mathrm{LT})/V(\mathrm{LT}) > 2$, which is considerably greater than the value of $\sigma(\mathrm{HT})/V(\mathrm{HT}) < 1$ reported.[24] These results should be strong evidence that the long axis static disorder of the charged up LT-phase should have the potential to continuously localize electrons. This conclusion is consistent with the theoretical prediction of the static disorder induced charge localization.[3–7] Detailed mapping of the transfer integral between two coaxial pentacene molecules sliding along the long axis (Figure 5, ref.[26] also elucidates the reason for the critical difference of localization between the two molecular configurations of the charged-up LT-phase and the discharged HT-phase. The first nodal plane appears with a minimum offset at 0.12 nm around which the sign and magnitude of the transfer integral are extremely sensitive to the precise position of the two molecules. In the HT-phase the maximum $\Delta C$ values including standard deviation at 0.08 (=0.03 + 0.05) nm is smaller than this critical offset, whereas that in the charged-up LT-phase at 0.35 (0.3 + 0.05) nm far exceeds it. Therefore, the fluctuation of the transfer integral of the charged-up LT-phase should be enough to induce the charge localization as we concluded.

Our results may be the first case to reveal the localization mechanism by using experimentally-observed realistic molecular configurations of pentacene polymorphs. They are also consistent with the polymorphic enantiotropy and the amorphous-like density of states observed in pentacene single crystals.[17,22,27] As the performance of newly proposed pentacene devices, such as singlet fission solar cells,[28] and solid-state masers[29] should strongly depend on the molecular configurations, we expect our findings will be useful in attempts to improve their performance.

In our present simulation, firstly molecular configurations were obtained by MD calculation with charges fixed to the randomly selected molecules, then their charge localizability of the configurations was evaluated by quantum chemical simulation. In the future, self-consistent combined MD and QC simulation is expected to elucidate the self-localization mechanism of charges at the interface between the semiconductor molecules and the dielectric surface.

In conclusion, by using in situ Raman spectroscopy, a clear reversible correlation between electron trapping and polymorph transformations was observed in highly crystalline zone-cast pentacene TFTs under prolonged gate bias stress, direct photoexcitation, and thermal annealing. Our combined MD and quantum-chemical simulations revealed that in molecular semiconductors, such as pentacene, trapped charges may be stabilized in certain intermolecular configurations with large, static long axis molecular displacements. If, as in the LT-phase of pentacene, a polymorph exists in which such large displacements are possible, the injection of at least locally large charge concentration into the organic semiconductor may trigger the local transformation between polymorphs. Our work identifies a new mechanism for charge trapping in molecular semiconductors with multiple polymorphs that should be taken into account when interpreting bias-stress-induced instabilities.

## Acknowledgements

The authors thank Prof. Richard Friend of the Cavendish Laboratory and Dr. D. Williams of Hitachi Cambridge Laboratory for their continuous support. They also thank the EPSRC/Cambridge Integrated Knowledge Centre for financial support (ROOT project). T.B.K. and C.M.D. thank Hitachi for funding. R.T.P. acknowledges EPSRC support. H.I. thanks JST-PRESTO "Molecular technology and creation of new functions" for financial support. M. A., T. B. K., and M. Y. thank Prof. Alberto Girlando of Parma University for fruitful discussion.

Received: August 5, 2014
Revised: September 30, 2014
Published online: November 10, 2014

[1] H. Minemawari, T. Yamada, H. Matsui, J. Tsutsumi, S. Haas, R. Chiba, R. Kumai, T. Hasegawa, *Nature* **2011***475*, 364.
[2] Y. Yuan, G. Giri, A. L. Ayzner, A. P. Zoombelt, S. C. B. Mannsfeld, J. Chen, D. Nordlund, M. F. Toney, J. Huang, Z. Bao, *Nat. Commun.* **2014**, doi:10.1038/ncomms4005.
[3] M. Unge, S. Stafstroem, *Synth. Metals* **2003**, *139*, 239.
[4] A. Troisi, G. Orlandi, *Phys. Rev. Lett.* **2006**, *96*, 086601.
[5] J.-D. Picon, M. N. Bussac, L. Zuppiroli, *Phys. Rev. B* **2007**, *75*, 235106.
[6] S. Ciuchi, S. Fratini, *Phys. Rev. B* **2011**, *83*, 081202(R).
[7] H. Ishii, K. Honma, N. Kobayashi, K. Hirose, *Phys. Rev. B* **2012**, *85*, 245206.
[8] H. Sirringhaus, T. Sakanoue, J.-F. Chang, *Phys. Status Solidi* **2012**, *B249*, 1655, and references there in.
[9] T. Heim, K. Lmimouni, D. Vuillaume, *Nano Lett.* **2004**, *4*, 2145.
[10] M. Tello, M. Chiesa, C. M. Duffy, H. Sirringhaus, *Adv. Funct. Mater.* **2008**, *18*, 3907.
[11] H. Sirringhaus, *Adv. Mater.* **2009**, *21*, 3859.
[12] T. Hallam, M. Lee, N. Zhao, I. Nandhakumar, M. Kemerink, M. Heeney, I. McCulloch, H. Sirringhaus, *Phys. Rev. Lett.* **2009**, *103*, 256803.
[13] W. C. Germs, K. Guo, R. A. J. Janssen, M. Kemerink, *Phys. Rev. Lett.* **2012**, *109*, 016601.
[14] M. Yoneya, M. Kawasaki, M. Ando, *J. Mater. Chem.* **2010**, *20*, 10397.
[15] C. M. Duffy, J. W. Andreasen, D. W. Breiby, M. M. Nielsen, M. Ando, T. Minakata, H. Sirringhaus, *Chem. Mater.* **2008**, *20*, 7252.
[16] T. Hallam, C. M. Duffy, T. Minakata, M. Ando, H. Sirringhaus, *Nanotechnology* **2009**, *20*, 025203.
[17] A. Brillante, I. Bilotti, R. G. D. Valle, E. Venuti, M. Masino, A. Girlando, *Adv. Mater.* **2005**, *17*, 2549.
[18] A. Brillante, I. Bilotti, R. G. D. Valle, E. Venuti, A. Girlando, M. Masino, F.Liscio, S. Milita, C. Albonetti, P. D'angelo, A. Shehu, F. Biscarini, *Phys. Rev. B* **2012**, *85*, 195308.
[19] C. B. Park, *Appl. Phys. Lett.100*, **2012**, 063306.
[20] E. F. Valeev, V. Coropceanu, D. A. da Silva Filho, S. Salman, J.-L. Bre'das, *J. Am. Chem. Soc.* **2006**, *128*, 9882.
[21] M. J. Powell, C. van Berkel, J. R. Hughes, *Appl. Phys. Lett.* **1989**, *54*, 1323.
[22] T. Siegrist, C. Besnard, S. Haas, M. Schiltz, P. Pattison, D. Chernyshov, B. Batlogg, C. Kloc, *Adv. Mater.* **2007**, *19*, 2079.
[23] P. W. Anderson, *Phys. Rev.* **1958**, *109*, 1492.
[24] A. Troisi, G. Orlandi, *J. Phys. Chem.* **2006**, *A110*, 4065.
[25] J.-F. Chang, T. Sakanoue, Y. Olivier, T. Uemura, M.-B. Dufourg-Madec, S. G. Yeates, J. Cornil, J. Takeya, A. Troisi, H. Sirringhaus, *Phys. Rev. Lett.* **2011**, *107*, 066601.
[26] A. Troisi, G. Orlandi, J. E. Anthony, *Chem. Mater.* **2005**, *17*, 5024.
[27] D. V. Lang, X. Chi, T. Siegrist, A. M. Sergent, A. P. Ramirez, *Phys. Rev. Lett.* **2004**, *93*, 086802.
[28] B. Eheler, M. W. B. Wilson, A. Rao, R. H. Friend, N. C. Greenham, *Nano Lett.* **2012**, *12*, 1053.
[29] M. Oxborrow, J. D. Breeze, N. M. Alford, *Nature* **2012**, *488*, 353.